PHYSICAL REVIEW C VOLUME 52, NUMBER 2 AUGUST 1995

New high-spin band structures in ^{184}Hg

J. K. Deng,* W. C. Ma,† J. H. Hamilton, A. V. Ramayya, J. Kormicki,‡
W. B. Gao,§ X. Zhao,‖ and D. T. Shi
Physics Department, Vanderbilt University, Nashville, Tennessee 37235

I. Y. Lee,¶ J. D. Garrett, N. R. Johnson, D. Winchell,** M. Halbert,
and C. Baktash
Physics Division, Oak Ridge National Laboratory, Oak Ridge, Tennessee 37831
(Received 26 August 1994; revised manuscript received 16 March 1995)

The high-spin states in ^{184}Hg have been investigated via the ^{154}Gd (^{32}S,4n) reaction at a beam energy of 160 MeV, with an array of Compton suppressed Ge detectors in the Spin Spectrometer at HHIRF. The ground state oblate band and excited prolate band were extended to 10^+ and 26^+, respectively, and seven new bands are observed. A new band with odd spins, 13 to 25, has a much larger moment of inertia than the other bands in ^{184}Hg. Two of the new bands feed the prolate excited band and are interpreted as quadrupole vibrational bands. Also, two new signature partner bands are observed for which the configuration of $\nu i_{13/2}f_{7/2}$ is proposed. The similarity of the band with odd spins to the band with intermediate deformation ($\beta_2 \sim 0.34$) in ^{186}Hg, and signature partner bands to the bands observed in 104 isotones ^{180}Os and ^{182}Pt, is discussed.

PACS number(s): 21.10.Re, 23.20.Lv, 27.70.+q, 29.30.Kv

INTRODUCTION

The light mass even-even mercury isotopes with $180 \leq A \leq 190$ exhibit a wide variety of shape-coexisting structures. In their ground states they exhibit small oblate deformation ($\beta_2 \sim -0.12$) and develop significant prolate deformation ($\beta_2 \sim 0.25$) in their low-lying excited states [1]. In Hg nuclei with $A \geq 189$, superdeformed excited bands with $\beta_2 \sim 0.45$ are observed [2]. In ^{186}Hg one of five recently discovered bands has the intermediate deformation of $\beta_2 \sim 0.34$ and is interpreted as a high-j ([651]1/2 $\otimes$ [514]7/2) or ([651]1/2 $\otimes$ [770]1/2) neutron configuration [3]. A similar negative parity band, but with smaller deformation, is seen in ^{184}Pt. The theoretical calculations [5] indicate that the band with intermediate deformation ($\beta_2 \sim 0.34$) seen in ^{186}Hg may also occur in ^{184}Hg. The level scheme of ^{184}Hg was previously studied by Cole *et al.* [4] from the decay of ^{184}Tl where the 0_2^+ band head and 2_2^+ to 8_2^+ members of the prolate excited band and the 2^+, 4^+, and 6^+ members of the oblate ground state band were observed. Ma *et al.* [5] (with a reaction similar to that used in the present work) identified levels in prolate bands up to 20^+. The mean lifetimes of the yrast levels from 8^+ to 18^+ in ^{184}Hg have been measured and the extracted values of deformation ($|\beta_2| \approx 0.26$) were found to be nearly constant, indicating a stable nuclear shape [5].

To obtain a systematic understanding of the structure of the nuclei in this region, the high-spin states in ^{184}Hg were investigated at the Holifield Heavy Ion Research Facility with the Spin Spectrometer (the first version of the Spin Spectrometer, before the recent upgrade is described in [6]).

I. EXPERIMENTAL PROCEDURES

The high-spin states of ^{184}Hg were populated by using the ^{156}Gd(^{32}S,4n) reaction with a beam energy of 160 MeV at the Holifield Heavy Ion Research Facility. The measured cross sections at the 155, 160, and 165 MeV show a maximum at 160 MeV for the yield of ^{184}Hg. A self-supporting ^{154}Gd target, with two foils stacked together and having a total thickness of 1085 μg/cm^2, was used. This target permitted the residual nuclei to recoil freely into vacuum with essentially their full initial velocity as determined by the reaction kinematics along the beam direction. The observed energies of the γ rays emitted from the moving residual nuclei were corrected for Doppler shift for each detector angle.

In-beam γ-ray coincidence events were detected with 18 Compton-suppressed Ge detectors in the Spin Spectrometer [6], which retained 54 of its NaI detectors to serve as sum-energy and multiplicity filters. The dis-

*Present address: Physics Department, Tsinghua University, Beijing, China.

†Present address: Physics Department, Mississippi State University, Mississippi State, MS 39762.

‡Also at UNISOR, ORISE, Oak Ridge, TN 37831; on leave from Institute of Nuclear Physics, Cracow, Poland.

§Present address: Medical Physics Division, University of Oklahoma, Norman, OK 73126.

‖Present address: Physics Department, Florida State University, Tallahassee, FL 32306.

¶Present address: Lawrence Berkeley Laboratory, Berkeley, CA 94720.

**Present address: Physics Department, University of Pennsylvania, Philadelphia, PA 19104.

tances between the target and the Ge detectors were 20 cm. To reduce the intensities of the x rays, stacked absorber foils of Ta (1.25 mm), Sn (0.25 mm), and Cu (0.125 mm) were used. During the analysis, gates on the coincidence-fold distribution were used to enhance the $4n$ reaction channel to high spin states in ^{184}Hg, but no gate on the total γ-ray energy was set. Approximately 150 million double or higher fold γ-ray coincidence events were accumulated on-line with the multiplicity distribution threshold of $k \geq 13$.

To obtain ratios of directional correlations from oriented nuclei (DCO) a two-dimensional matrix was created from the coincidence data with γ rays in the six detectors close to 0° and 180° on the x axis and those in the twelve detectors close to 90° on the y axis. About 70 million double coincidence events were obtained in the DCO two-dimensional matrix from the two groups of detectors with the gate set at $k \geq 13$. The DCO [7] ratios were used to establish the spins of the levels and multipolarities of the transition. For the geometry in this experiment, a stretched quadrupole transition has a DCO ratio of 1.0 while a stretched dipole gives 0.7.

II. RESULTS

The new transitions in ^{184}Hg determined in the present work were identified and placed in the level scheme by their coincidence relationships with each other and with the previously known γ rays [4, 5]. The level scheme of ^{184}Hg proposed from the present work is shown in Fig. 1. Bands 3 and 7 were previously known from Ref. [5]. Seven new rotational bands, i.e., bands 1, 2, 4, 5, 6, 8, and 9, were observed for the first time.

The spin values have been assigned for many energy levels based on the DCO ratios, as listed in Table I. All the transitions placed in rotational bands have stretched quadrupole character. The stronger interband transitions from band 6 to band 7, as well as to other low spin structures, show stretched dipole character, which suggests odd spin for band 6. The DCO ratios for 789.5-, 809.2-, and 650.2-keV interband transitions have been determined to be in the range of 0.6 to 0.7 (see Table I). So these interband transitions from band 8 to band 7 and from band 9 to band 8 carry only $1\hbar$ angular momentum, which establishes that band 8 has odd spin and band 9

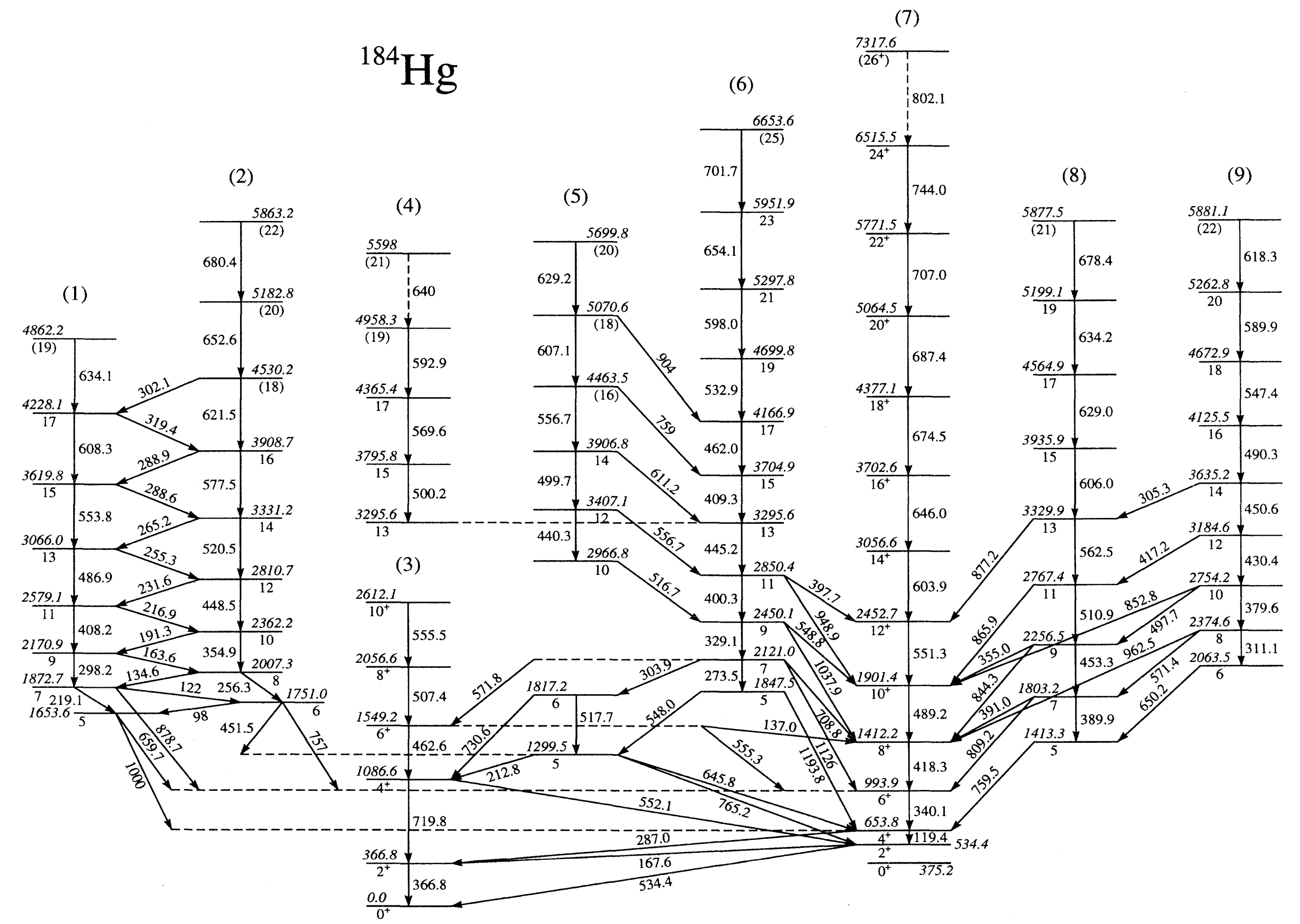

FIG. 1. Proposed level scheme for ^{184}Hg.

TABLE I. Energies, intensities, DCO ratios, and assignments in ^{184}Hg.

E_γ(keV)[a]	E_{level}(keV)	I[b]	Assignment	DCO ratio	Gate[c]
98[d]	1751.0	11(1)	$6 \to 5$		
119.4(3)	653.8	1.1(2)	$4 \to 2$	1.10(48)	sum[g]
122[d]	1872.7	6(1)	$7 \to 6$		
134.6(1)	2007.3	5.1(3)	$8 \to 7$	0.78(18)	219
137.0(1)[d]	1549.2	1.4(2)	$6^+ \to 8^+$		
163.6(1)[d]	2170.9	2.4(2)	$9 \to 8$		
167.6(2)	534.4	2.5(7)	$2^+ \to 2^+$	1.32(52)	367
191.3 (1)	2362.2	3.2(2)	$10 \to 9$	0.65(17)	298
212.8(3)	1299.5	1.3(4)	$5 \to 4^+$	0.73(14)	720
216.9(1)[e]	2579.1	1.5(2)	$11 \to 10$		
219.1(1)	1872.7	3.3(1)	$7 \to 5$	0.84(16)	298
231.6(1)	2810.7	0.9(1)	$12 \to 11$	0.74(25)	521
255.3(1)[d,e]	3066.0	0.6(2)	$13 \to 12$		
256.3(1)[d,e]	2007.3	0.7(1)	$8 \to 6$		
265.2(2)	3331.2	0.3(1)	$14 \to 13$	0.64(10)	578
273.5(1)	2121.0	4.9(1)	$7 \to 5$	0.96(5)	329
287.0(1)	653.8	83.3(2)	$4^+ \to 2^+$	1.02(1)	367
288.6(2)[d,e]	3619.8	0.2(1)	$15 \to 14$		
288.9(2)[d,e]	3908.7	0.2(2)	$16 \to 15$		
298.2(1)	2170.9	1.7(1)	$9 \to 7$	0.88(15)	219
302.1(2)[d]	4530.2		$18 \to 17$		
303.9(1)	2121.0	3.2(1)	$7 \to 6$	0.77(5)	329
305.1(6)	3635.2	1.6(1)	$14 \to 13$	0.58(11)	563
311.1(1)	2374.6	1.0(1)	$8 \to 6$	1.17(13)	380
319.4(2)[d]	4228.1	0.2(2)	$17 \to 16$		
329.1(1)	2450.1	11.5(2)	$9 \to 7$	0.94(5)	287
340.1(1)	993.9	72.1(1)	$6^+ \to 4^+$	0.97(1)	287
354.9(1)	2362.2	2.2(1)	$10 \to 8$	0.87(15)	287
355.0(3)[e]	2256.5	1.1(1)	$9 \to 10$		
366.8(1)	366.8	100.0	$2^+ \to 0^+$	1.00(1)	287
379.6(1)	2754.2	4.0(1)	$10 \to 8$	1.05(7)	429
389.9(1)	1803.2	3.1(1)	$7 \to 5$	1.05(10)	287
391.0(2)[d,e]	1803.2	0.5(1)	$7 \to 8$		
397.7(3)[d]	2850.4	0.4(1)	$11 \to 12^+$		
400.3(1)	2850.4	14.5(2)	$11 \to 9$	1.10(4)	329
408.2(1)	2579.1	3.5(4)	$11 \to 9$	1.09(15)	298
409.3(1)	3704.9	8.6(2)	$15^+ \to 13^+$	0.91(4)	446
417.2	3184.6	1.6(1)	$12 \to 11$	0.51(9)	450
418.3(1)	1412.2	64.0(5)	$8^+ \to 6^+$	0.99(1)	340
430.4(1)	3184.6	4.3(1)	$12 \to 10$	0.89(6)	454
440.3(1)	3407.1	1.2(1)	$12 \to 10$	0.83(13)	329
445.2(1)	3295.6	11.1(2)	$13 \to 11$	1.08(4)	401
448.5(1)	2810.7	2.5(2)	$12 \to 10$	0.91(12)	521
450.6(1)	3635.2	4.3(1)	$14 \to 12$	1.08(8)	429
451.5(2)[d]	1751.0	0.7(2)	$6 \to 5$		
453.3(1)	2256.5	4.2(1)	$9 \to 7$	0.93(13)	340
462.0(1)	4166.9	6.5(4)	$17 \to 15$	1.08(7)	446
462.6(1)[f]	1549.2	2.1(5)	$6 \to 4$	0.98(14)	720
486.9(1)	3066.0	1.1(2)	$13 \to 11$	0.85(13)	408
489.2(1)	1901.4	46.0(4)	$10 \to 8$	0.95(2)	418
490.3(1)	4125.5	3.2(4)	$16^+ \to 14^+$	1.12(11)	450
497.7(1)	2754.2	2.2(1)	$10 \to 9$	0.54(14)	454
499.7(1)	3906.8	0.9(1)	$14 \to 12$	0.89(7)	440
500.2(1)	3795.8	2.5(1)	$15 \to 13$	0.95(13)	446
507.4(1)	2056.6	2.2(6)	$8 \to 6$	0.99(9)	462
510.9(1)	2767.4	6.2(1)	$11 \to 9$	1.09(8)	454
516.7(3)[e,f]	2966.8	3.5(3)	$10 \to 9$		
517.7(3)[f]	1817.2	1.0(4)	$6 \to 5$	1.08(31)	304
520.5(1)	3331.2	1.4(5)	$14 \to 12$	0.98(11)	448

Table I. *(Continued)*.

E_γ(keV)[a]	E_{level}(keV)	I[b]	Assignment	DCO ratio	Gate[c]
532.9(1)	4699.8	4.1(3)	$19 \rightarrow 17$	1.03(8)	462
534.4(1)	534.4	7(2)	$2^+ \rightarrow 0^+$	0.94(14)	340
547.4(1)	4672.9	2.9(5)	$18 \rightarrow 16$	1.19(15)	450
548.0(1)[f]	1847.5	3.9(6)	$5 \rightarrow 5$	1.08(10)	273
548.8(2)[e,f]	2450.1	4.3(2)	$9 \rightarrow 10^+$		
551.3(1)	2452.7	31.0(4)	$12^+ \rightarrow 10^+$	0.99(2)	489
552.1(1)	1086.6	4.9(5)	$4^+ \rightarrow 2^+$	1.19(12)	462
553.8(1)	3619.8	0.8(3)	$15 \rightarrow 13$	1.13(17)	408
555.3(3)[e,f]	1549.2	5(2)	$6^+ \rightarrow 6^+$		
555.5(1)[d,e]	2612.1		$10^+ \rightarrow 8^+$		
556.7(1)[e,f]	4463.5	1.1(3)	$(16) \rightarrow 14$		
556.7(3)[e,f]	3407.1	1.8(4)	$12 \rightarrow 11$		
562.5(1)	3329.9	2.8(1)	$13 \rightarrow 11$	0.91(9)	511
569.6(1)	4365.4	2.2(2)	$17 \rightarrow 15$	0.88(15)	446
571.4(1)	2374.6	2.0(2)	$8 \rightarrow 7$	0.81(11)	390
571.8(1)	2121.0	4.5(3)	$7 \rightarrow 6$	0.72(17)	329
577.5(1)	3908.7	0.7(4)	$16 \rightarrow 14$	0.98(13)	521
589.9(1)	5262.8	2.5(4)	$20 \rightarrow 18$	1.05(13)	547
592.9(1)	4958.3	1.4(1)	$19 \rightarrow 17$	0.98(13)	446
598.0(1)	5297.8	2.6(2)	$21 \rightarrow 19$	1.02(12)	532
603.9(1)	3056.6	23.5(4)	$14 \rightarrow 12$	1.11(5)	551
606.0(1)	3935.9	2.9(2)	$15 \rightarrow 13$	1.15(16)	563
607.1(1)	5070.6	1.2(1)	$(18) \rightarrow (16)$	0.95(15)	557
608.3(1)	4228.1	0.6(6)	$17 \rightarrow 15$	0.81(31)	554
611.2(2)	3906.8	1.6(1)	$14 \rightarrow 13$	0.82(24)	446
618.3(1)[d]	5881.1	1.3(2)	$(22) \rightarrow 20$		
621.5(1)[d]	4530.2	0.8(8)	$(18) \rightarrow 16$		
629.0(1)	4564.9	1.2(1)	$17 \rightarrow 15$	1.05(23)	606
629.2(1)	5699.8	0.7(2)	$(20) \rightarrow (18)$	0.89(21)	608
634.1(2)[d]	4862.2		$(19) \rightarrow (17)$		
634.2(1)	5199.1	0.8(2)	$19 \rightarrow 17$	0.66(13)	629
640[d]	5598		$(21) \rightarrow (19)$		
645.8(1)[d]	1299.5	1.7(6)	$5 \rightarrow 4^+$		
646.0(1)	3702.6	11.5(2)	$16^+ \rightarrow 14^+$	0.98(6)	604
650.2(1)	2063.5	1.4(1)	$6 \rightarrow 5$	0.72(9)	380
652.6(1)[d]	5182.8		$(20) \rightarrow (18)$		
654.1(1)	5951.9	1.7(1)	$23 \rightarrow 21$	0.70(13)	sum[g]
659.7(2)[d]	1653.6	1.1(2)	$5 \rightarrow 6^+$		
674.5(1)	4377.1	5.4(2)	$18^{18} \rightarrow 16$	1.03(5)	sum[g]
678.4(2)[d]	5877.5	0.3(1)	$(21) \rightarrow 19$		
680.4(2)[d]	5863.2		$(22) \rightarrow (20)$		
687.4(1)	5064.5	2.6(1)	$20^+ \rightarrow 18^+$	1.02(7)	sum[g]
701.7(2)[d]	6653.6	0.6(1)	$(25) \rightarrow 23$		
707.0(1)	5771.5	1.2(1)	$22^+ \rightarrow 20^+$	0.89(19)	sum[g]
708.8(1)	2121.0	3.7(2)	$7 \rightarrow 8^+$	0.82(6)	sum[g]
719.8(1)	1086.6	3.3(3)	$4^+ \rightarrow 2^+$	1.09(14)	367
730.6(1)	1817.2	1.6(7)	$6 \rightarrow 4^+$	0.76(11)	304
744.0(1)	6515.5	0.7(1)	$24^+ \rightarrow 22^+$	1.02(21)	sum[g]
757[d]	1751.0	0.4(2)	$6 \rightarrow 6^+$		
759[d]	4463.5	0.6(1)	$(16) \rightarrow 15$		
759.5(1)	1413.3	5.6(1)	$5 \rightarrow 4^+$	0.72(7)	287
765.2	1299.5	3(1)	$5 \rightarrow 2^+$		
802.1(2)[d]	7317.6		$(26^+) \rightarrow 24^+$		
809.2(1)	1803.2	4.4(2)	$7 \rightarrow 6^+$	0.61(8)	340
844.3(1)	2256.5	3.2(2)	$9 \rightarrow 8^+$	0.75(12)	418
852.8(2)	2754.2	1.4(2)	$10 \rightarrow 10^+$	1.20(30)	489
865.9(2)[d]	2767.4	1.0(1)	$11 \rightarrow 10^+$		
877.2(2)[d]	3329.9	1.0(1)	$13 \rightarrow 12^+$		

TABLE I. (*Continued*).

878.7(2)	1872.7	1.4(4)	$7 \to 6^+$	0.83(20)	340
904[d]	5070.6	0.4(1)	$(18) \to 17$		
948.9(1)	2850.4	1.3(3)	$11 \to 10^+$	0.61(16)	489
962.5(2)	2374.6	1.1(1)	$8 \to 8^+$	0.92(25)	418
1000[d]	1653.6	0.5(1)	$5 \to 4^+$		
1037.9(2)	2450.1	2.3(2)	$9 \to 8^+$	0.69(19)	418
1126(1)[d]	2121.0	0.3(1)	$7 \to 6^+$		
1193.8(2)	1847.5	1.5(2)	$5 \to 4^+$	0.56(9)	sum[g]

[a] γ-ray energies were obtained from gated coincidence spectra.
[b] Transition intensities were mostly obtained from gated coincidence spectra and were normalized to the 366.8 keV transition.
[c] DCO ratios were obtained from these gated spectra.
[d] Very low intensity γ transition; no intensity and/or DCO ratio determination was possible.
[e] Complex line, no intensity and/or DCO ratio determination was possible.
[f] Complex line, intensity estimated from coincidence spectra.
[g] Sum of several gated spectra.

has even spin. These results are consistent with the new results [3] for the similar bands (band 4 and band 5) in ^{186}Hg. However, the parities of these new bands cannot be determined uniquely from the data presented here.

After the spin assignments had been made from the DCO ratios, corrections for the total internal conversion of the transitions were made using the relation $I(E_\gamma) = A(E_\gamma)[1+\alpha(E_\gamma)]$, where $A(E_\gamma)$ is relative γ-ray intensity and $\alpha(E_\gamma)$ is the total conversion coefficient. The total internal conversion coefficients were obtained from Ref. [8]. The strong interband transitions were assumed to be of $M1$ character. Then the relative intensities of the new transitions corrected for total internal conversion, based on measured DCO ratios, were calculated by balancing the intensities in the level scheme. The γ-ray energies, intensities, assignments, and DCO ratios are given in Table I.

Band 3 is built on an oblate ground state having $\beta_2 \sim 0.15$ [5]. The 575.6- ($8^+ \to 6^+$) and 691-keV ($10^+ \to 8^+$) transitions tentatively placed by Ma *et al.* [5] were not observed in the present work. Instead three transitions of energies 462.6, 507.4, and 555.5 keV are placed in the level scheme on the top of band 3, as shown in Fig. 1.

The excited prolate band 7 with $\beta_2 \sim 0.26$ [5], which coexists with the oblate ground-state band (band 3), was extended to spin (26^+). The new sequence of transitions established presently for band 7 changes the sequence previously reported [5]. It includes new transitions with energies 687.4 keV, 707.0 keV, and 744.0 keV, and at the same time excludes transitions 761 keV and 809 keV tentatively placed in Ref. [5]. The new 687.4-keV transition is inserted into this band as the $20^+ \to 18^+$ transition. That is illustrated in Fig. 2 where spectra gated on the new 687.4 keV transition and its neighboring transitions, 674.5 keV and 646.0 keV in band 7, show the coincidence relationships of transitions within this band. The new 707.0- and 744.0-keV transitions are located as $24^+ \to 22^+$ and $22^+ \to 20^+$ members of band 7, respectively, based on their relative coincidence relations and relative intensities. The tentative assignment of the 802-keV transition as the $26^+ \to 24^+$ member is based on the following considerations. The 802-keV transition is visible in a sum of spectra gated on the clean transitions which are located high in the band. Also, most of the low-lying members of the discussed yrast band can be found in the spectrum gated on the 802-keV transition despite poor statistics. The 809-keV and 761-keV transitions which were tentatively assigned as (24^+) $\to$ (22^+) and (22^+) $\to$ (20^+) transitions in [5] feed the 6^+ and 4^+ levels of band 7, respectively, as the interband transitions. In the present data, the 119-keV transition from $4_2^+ \to 2_2^+$ can be observed, although it is weak because of its large internal conversion. The $2_2^+ \to 0_2^+$ seen in decay work [4] is still not observed in our in-beam data.

Band 6 is the second strongest populated band in the ^{184}Hg level scheme, with an intensity of ~14% for the 400-keV transition in the lower part in this band. The placements of the transitions in this band were established by the coincidence relations of the γ rays with each other and by their intensities, as illustrated in Fig. 3,

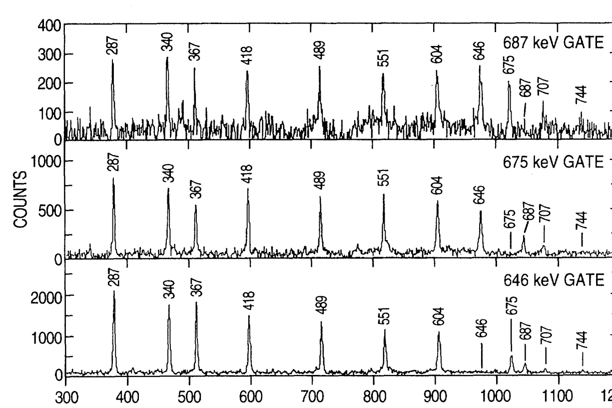

FIG. 2. Spectra showing coincidence relations within band 7 in ^{184}Hg. Gates on the new 687-keV γ ray and its neighboring transitions, 675 and 646 keV, are shown.

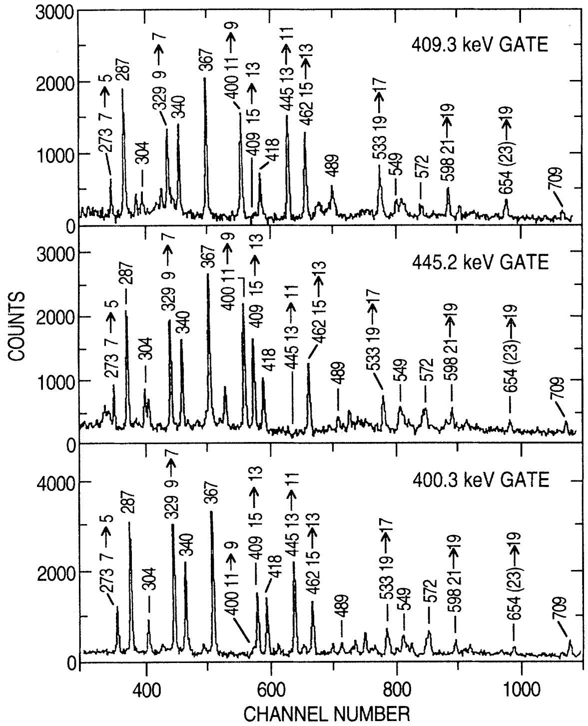

FIG. 3. Spectra showing coincidence relations within band 6 in ^{184}Hg. Gates on the 400-, 445-, and 409-keV transitions. The in-band transitions are marked with energies and have spins of initial and final states, while interband transitions are marked with energies only.

where spectra gated on 400.3-keV, ($11 \to 9$), 445.2-keV ($13 \to 11$) and 409.3-keV ($15 \to 13$) transitions are shown. Also, several interband transitions were found depopulating this band and feeding band 7 and other low spin states in ^{184}Hg. The DCO ratios of the transitions to band 7 establish odd spins for band 6.

For bands 8 and 9, the intensities of band-head transitions are about 5% and 4%, respectively. These bands feed only into the prolate deformed band, that is, band 7. The spectra gated on the 563-keV transition inside band 8 and on the 759-keV transition linking to band 7, as shown in Fig. 4, demonstrate the coincidence relations of transitions in band 8.

Bands 4 and 5 are very weak, with band-head intensities $\leq$2.5% in band 4 and $\sim$1% in band 5. Even though some of the transitions are deduced from γ-ray multiplets, the coincidence relations of these transitions are clearly identified. Both bands 4 and 5 populate only the odd-spin band 6, which has a large moment of inertia. Band 5 is particularly unusual in that it feeds several members of band 6, including high spin members with large moments of inertia and low spin members with smaller moments of inertia.

Bands 1 and 2 have the intensities of band-head transitions around $\sim$ 2–3% of the $2^+ \to 0^+$ transition in the ground state band. They consist of stretched $E2$ tran-

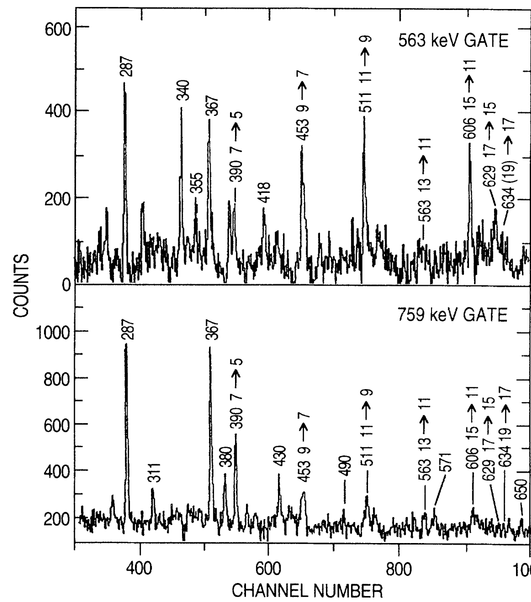

FIG. 4. Spectra showing coincidence relations within band 8 gated on the 759- and 563-keV transitions. The transitions marked with energies and the spin assignments of initial and final states are transitions in the band, and those marked with only energies are transitions in other bands.

sitions with $M1$ intraband transitions connecting each other. Although the transitions linking these two bands with other levels in ^{184}Hg are weak (relative intensity <1%), the coincidence spectra indicated their relations to low spin structures in band 3 and band 7. Figure 5 shows linking of transitions in bands 1 and 2 with the transition 340.1 keV in band 7, and transitions 366.8 keV and 287.0 keV linked to band 3.

III. DISCUSSION

The characteristics of bands in ^{184}Hg will be discussed and compared with characteristics of similar bands in

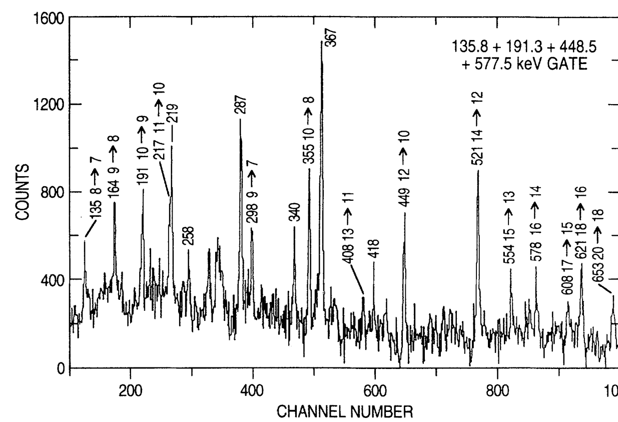

FIG. 5. The coincidence spectra obtained by gating on the 135.8-, 191.3-, 448.5-, and 577.5-keV transitions in bands 1 and 2 and summing them.

^{186}Hg and other nuclei with N=104.

Band 7. The rotational properties of the high spin members of the prolate deformed band (band 7), are similar to the properties of yrast band in ^{186}Hg [3]. The yrast bands are interpreted to have the configuration $\nu i_{13/2}, \pi h_{9/2}$ and $\pi i_{13/2}$ quasiparticle excitations coupled to the prolate core [3]. For bands in ^{184}Hg and ^{186}Hg, the moment of inertia (J_1) as a function of the rotational energy is shown in Fig. 6. From Fig. 6 one can see that the moment of inertia (J_1) varies similarly in these two nuclei and exhibits smooth increase and upbending. The aligned angular momentum $i(\hbar)$ versus the rotational energy $\hbar\omega$ for bands in ^{184}Hg is shown in Fig. 7. To calculate the aligned angular momentum, the first four members of the prolate band were used as the reference band. The parameters J_1 and J_2 were calculated to be 27.6 $\hbar^2$/MeV and 187.79 $\hbar^4$/MeV^2, respectively. A gain in alignment of $\sim 4\hbar$ at the crossing frequency of $\sim$0.34 MeV is in qualitative agreement with the theoretical calculation for the $i_{13/2}$ rotation-aligned neutron-band coupled to the prolate band, even though the gain in alignment is smaller than theoretically expected. Figure 7 also shows the behavior of the alignment of other bands in ^{184}Hg.

Band 6. Lifetime data of a similar band in ^{186}Hg (band 3) established this band to have a deformation midway between normal and superdeformation [3]. This new intermediate deformation was interpreted as an excitation of two quasineutrons, either the $\nu([651]1/2 \otimes [514]7/2)$ or the $\nu([651]1/2 \otimes [770]1/2)$ configuration, or a mixture of both of these configurations [5]. In Fig. 8 a crossing between bands 6 and 7 at $\hbar\omega$ $\sim$0.32 MeV can be seen. Figure 6 shows the kinetic moment of inertia of band 6 in ^{184}Hg. The kinetic moment of inertia (J_1) of this band 6 in the spin range 13–23 is high compared to the pro-

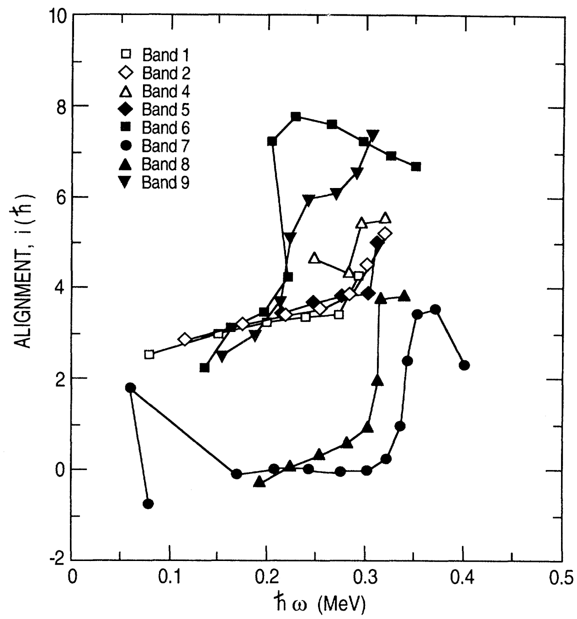

FIG. 7. Experimental alignment i as a function of rotational frequency $\hbar\omega$ in ^{184}Hg. The reference parameters are J_0 = 27.64$\hbar^2$/MeV and J_1 = 187.79$\hbar^4$/MeV^2.

late band 7 and is very similar in magnitude to band 3 in ^{186}Hg. The parity of band 3 in ^{186}Hg has been established to be negative. The alignment patterns for band 6 in ^{184}Hg and band 3 in ^{186}Hg are different from the alignment for prolate bands in these two nuclei. Band 6 in ^{184}Hg becomes yrast above $I \sim 19$ (see Fig. 1), which

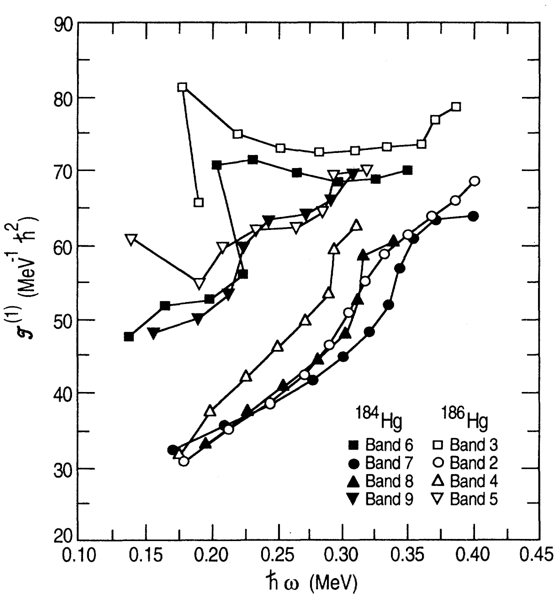

FIG. 6. Comparison of the kinetic moment of inertia $J^{(1)}$ for bands 6, 7, 8, and 9 in ^{184}Hg and for similar bands in ^{186}Hg.

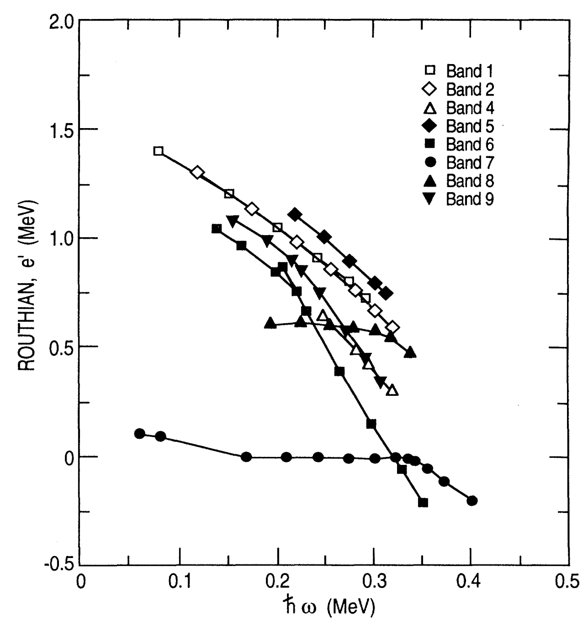

FIG. 8. Experimental Routhians e' as a function of rotational frequency $\hbar\omega$ in ^{184}Hg. The reference parameters are J_0 = 27.64$\hbar^2$/MeV and J_1 = 187.79$\hbar^4$/MeV^2.

is a little higher than in the case of ^{186}Hg [3]. Both of these similar bands in ^{184}Hg and ^{186}Hg have odd spins, but band 6 in ^{184}Hg seems to start with spin 5, while band 3 in ^{186}Hg starts with a spin and parity of 11^-. Also, in band 6 of ^{184}Hg the moment of inertia below spin 13 (see Fig. 6) is a different from that of the higher spin states, while the moment of inertia of band 6 above spin 11 is similar to that of band 3 in ^{186}Hg with negative parity. This indicates a change of structure around spin 13. The high spin members ($\geq$13) of band 6 have a different structure from that of low spin memers (<13). It is possible that what we discuss here as band 6 in fact may represent two bands with different structure. At the moment, the configuration for this odd-spin band in ^{184}Hg remains unclear.

Bands 8 and 9. The properties of these two bands in ^{184} Hg, including their feeding the prolate band (band 7) and the behavior of their moments of inertia (J_1) (see Fig. 6), are very similar to those of bands 4 and 5, respectively, in ^{186}Hg. Figure 7 shows that band 8 in ^{184}Hg has an alignment pattern very much like that of the yrast band and has a crossing at about 0.32 MeV. Band 9 has a much higher spin alignment than band 8, and has two crossings occurring at frequencies of approximately 0.23 and 0.30 MeV (see Fig. 8). DCO ratios of the 759.5- and 809.2-keV linking transitions between bands 8 and 7 show that band 8 has odd spins, contrary to the original assignment of even spins to band 4 of ^{186}Hg [3]. Recent internal conversion electron studies for the linking transitions between band 4 and the prolate ground band in ^{186}Hg [3] indicate that the linking transitions may be a mixture of $M1$ and $E2$ radiation, and so band 4 in ^{186}Hg may also be interpreted as an odd-spin band starting with spin of 3^+. This conclusion lets these similar bands in ^{184}Hg and ^{186}Hg have consistent spin assignments. Band 8 in ^{184}Hg most likely has positive parity as an analogue with band 4 in ^{186}Hg. However, the state with spin 3 has not been observed in band 8 in ^{184}Hg. Bands 8 and 9 may represent collective quadrupole excitations built on the excited prolate deformed shape. More precise data are needed to establish the exact nature of these bands.

Bands 1 and 2. The structures of bands 1 and 2 in ^{184}Hg show that these two bands are signature partners that show no signature splitting of their Routhians (see Fig. 8). Bands 1 and 2 are similar in transition energies to the two signature partner bands built on the $K^\pi = 8^-$ isomer ($T_{1/2}$ = 82 μs) in ^{186}Hg [3], but in ^{184}Hg transitions to the low spin structures in bands 3 and 7 are observed, which indicate a different configuration in ^{184}Hg compared to ^{186} Hg. Similar bands have also been observed in some other nuclei with neutron number N = 104. For example, bands labeled 3 and 4 in ^{182}Pt [9] and the bands labeled as $(-,1)_1$ and $(-,0)_1$ in ^{180}Os [10].

These bands in ^{180}Os and ^{182}Pt, built on an $I = 7$ spin state, have similar structure and no signature splitting in their Routhians. The bands labeled 3 and 4 in ^{184}Hg may be similar to the bands observed in ^{182}Pt and in ^{180}Os. Their moments of inertia (J_2) are compared in Fig. 9, showing that all these bands exhibit a similar alignment pattern below the crossing frequency. A band crossing occurs at $\hbar\omega \sim 0.27$ MeV in ^{184}Hg and ^{180}Os, while the

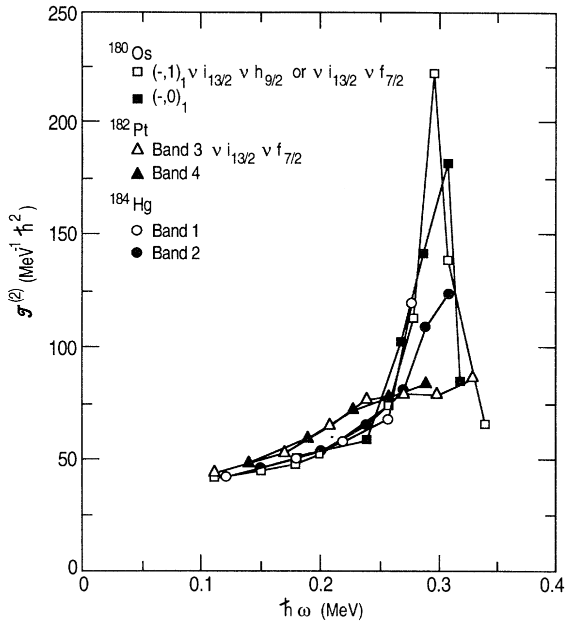

FIG. 9. Dynamical moments of inertia (J_2) of bands in ^{184}Hg and also in ^{180}Os, ^{182}Pt.

bands in ^{182}Pt show only a gradual gain in alignment in that frequency region.

These bands are considered to have a quasiparticle configuration of $[633]7/2^+ \otimes [514]7/2^-$ [9, 10]. The measured $B(M1)/B(E2)$ ratios for bands 1 and 2 in ^{184}Hg are compared below with calculated ones. For calculation the simplified model of Ref. [11] has been used. In this model the ratio $B(M1)/B(E2)$ is defined for an axially symmetric nucleus as

$$\frac{B(M1, I \to I-1)}{B(E2, I \to I-2} = \frac{16}{5Q_0^2}\left(1 - \frac{K^2}{(I-1/2)^2}\right)^{-2}\left(\frac{K}{I}\right)^2 \times[(g_1 - g_{R})(\sqrt{I^2-K^2} - i_1) - (g_2 - g_{R})i_2]^2,$$

where Q_0 is the quadrupole moment defined [12, 13] by the relation

$$Q_0 = 0.0109 Z A^{2/3}\beta_2(1 + 0.36\beta_2)[eb].$$

Assuming a $\beta_2 \simeq 0.25$, one calculates Q_0 of 7.69[eb]. The values of K and i_1 are given by the spin components of the quasiparticle on the symmetry axis and on the rotational axis, respectively. The band head spin of 7 is used for K. The i_1 and i_2 values are determined by the alignment of angular momentum of these bands, which has a total value of about 3$\hbar$, as measured from Fig. 7. Assuming equal contributions of both neutrons to the alignment, one gets the value of 1.5$\hbar$ for i_1 and i_2. The gyromagnetic ratios g_1 and g_2 are those of the quasiparticles. For the $i_{13/2}$ neutron intruder orbital, the Schmidt value of g_j as defined in Ref. [12] for deformed nuclei is a rather accurate estimate of g_1 and g_2 and is calculated

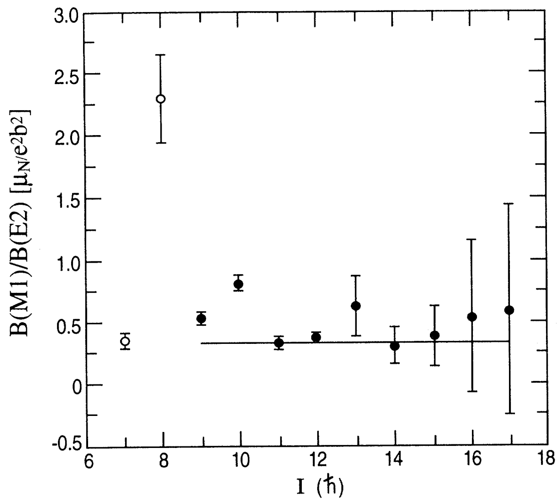

FIG. 10. Experimental and calculated $B(M1)/B(E2)$ ratios for the states in bands 1 and 2 of ^{184}Hg. Closed symbols: states assigned to band 1 and 2; open symbols: states not assigned to band 1 or 2. The solid line is the calculated value of $B(M1)/B(E2)$.

using the relationship

$$g_1 = g_2 = g_j = g_l + \frac{g_s - g_l}{2l+1}.$$

Using $g_s = 0.6g_s(\text{free})$ and $g_s(\text{free}) = -3.826$ for $i_{13/2}$ neutrons, g_1 has been calculated to be 0.18. The gyromagnetic ratio g_R is that of the core which is approximated by $g_R = Z/A = 0.35$.

Assuming all the $\Delta I = 1$ transitions are pure $M1$ transitions, the $B(M1)/B(E2)$ value calculated using the above parameters is about 0.3. Figure 10 shows the experimental and calculated $B(M1)/B(E2)$ values and their good agreement. The result for the state with spin 8^+ at 2007.3 keV, shown as an open circle in Fig. 10, suggests that the spin-6 state at 1751.0 keV most probably is not a member of band 2. Assuming this, the two bands (bands 1 and 2) most probably have the same configuration as the similar bands in ^{180}Os and ^{182}Pt.

IV. CONCLUSIONS

In summary, seven new bands have been observed in ^{184}Hg, and the previously known oblate ground-state (band 3) and excited prolate (band 7) bands were extended to 10^+ and 26^+, respectively. One of the new bands (band 6) has a moment of inertia similar to that of the band in ^{186}Hg with intermediate deformation $\beta_2 \sim 0.35$ while two other new bands (bands 8 and 9) are assigned quadrupole vibrational structure. The two signature partner bands (bands 1 and 2) have the same configurarion of $\nu i_{13/2}\nu f_{7/2}$ and are similar to the bands in ^{180}Os and ^{182}Pt. The nature of the other two new high-spin bands has not been determined.

ACKNOWLEDGMENTS

Work at Vanderbilt is supported in part by the U.S. Department of Energy under Grant No. DE-FG05-88ER40407. Oak Ridge National Laboratory is managed by Martin Marietta Energy Systems for the U.S. Department of Energy under Contract No. DE-AC05-84OR21400.

[1] J. H. Hamilton, in *Treatise on Heavy-Ion Science*, edited by D. A. Bromley (Plenum, New York, 1988), Vol. 8, p. 2.

[2] R. V. F. Janssens and T. L. Khoo, Annu. Rev. Nucl. Part. Sci. **41**, 321 (1991).

[3] W. C. Ma, J. H. Hamilton, A. V. Ramayya, L. Chaturvedi, J. K. Deng, W. B. Gao, Y. R. Yiang, J. Kormicki, X. W. Zhao, N. R. Johnson, J. D. Garrett, I. Y. Lee, C. Baktash, F. K. McGowan, W. Nazarewicz, and R. Wyss, Phys. Rev. C **47**, R5 (1993).

[4] J. D. Cole *et al.*, Phys. Rev. Lett. **37**, 1185 (1976).

[5] W. C. Ma, A. V. Ramayya, J. H. Hamilton, S. J. Robinson, J. D. Cole, E. F. Zganjar, E. H. Spejewski, R. Bengstsson, W. Nazarewicz, and J.-Y. Zhang, Phys. Lett. **167B**, 277 (1986).

[6] M. Jääskeläinen, D. G. Sarantites, R. Woodward, F. A. Dilmanian, J. T. Hood, and R. Jääskeläinen, D. C. Hensley, M. L. Halbert, and J. H. Barker, Nucl. Instrum. Methods Phys. Res. **204**, 385 (1983).

[7] K. S. Krane, R. M. Steffen, and R. M. Wheller, Nucl. Data Tables **A11**, 351 (1973).

[8] J. D. Cole, W. Lourens, J. H. Hamilton, and B. Van Nooijen, *Graphical Representation of K^- Shell and Total Internal Conversion Coefficients from Z = 30-104* (Delft University Press, Delft, 1984).

[9] D. G. Popescu, W. Schnitz, J. K. Johanson, G. Kajrys, D. D. Rajnauth, J. C. Waddington, M. P. Carpenter, V. P. Janzen, L. L. Riedinger, S. Moaro, and S. Pilotte, "Progress Report on Nuclear Spectroscopic Studies," [University of Tennessee Report No. 88-03, 1988, (unpublished), p. 27].

[10] A. Neskakis, R. M. Leidev, G. Sletten, and J. D. Garrett, Phys. Lett. **118B**, 49 (1982).

[11] F. Dönau and S. Frauendorf, in *Proceedings of the Conference on High Angular Momentum Properties of Nuclei*, edited by N. R. Johnson (Harwood Academic, New York, 1983), p. 143.

[12] K. E. G. Löbner, M. Vetter, and V. Hönig, Nucl. Data Tables **A7**, 495 (1970).

[13] W. Nazarewicz, R. Wyss, and A. Johnson, Nucl. Phys. **A503**, 285 (1989).